JOURNAL OF Materials CHEMISTRY

# Synthesis and magnetic susceptibility of the rutile phase $MnTaO_4$

**Jekabs Grins,[a] Saeid Esmaeilzadeh,[a] Magnus Andersson[b] and Andrzej Morawski[c]**

[a]*Department of Inorganic Chemistry, Arrhenius Laboratory, Stockholm University, SE-106 91 Stockholm, Sweden. E-mail: mat@inorg.su.se*
[b]*Department of Solid State Physics, Kungliga Tekniska Högskolan, SE-100 44 Stockholm, Sweden*
[c]*Polish Academy of Sciences, 01-142 Warsaw, Poland*

***Received 31st January 2000, Accepted 27th June 2000***
***Published on the Web 4th August 2000***

The $Mn^{3+}$-containing oxide $MnTaO_4$ was synthesized at 1050 °C and 2 kbar partial oxygen gas pressure. It has a rutile-type structure, space group $P4_2/mnm$, with $a=4.7189(3)$, $c=2.9843(3)$ Å, and a statistical distribution of Mn/Ta. The structure was refined by the Rietveld method using both X-ray and neutron powder diffraction. The refinements, and energy-dispersive X-ray microanalysis, indicate that the phase may contain a small amount of $Mn^{4+}$ and have the actual composition $Mn_{1.08(2)}Ta_{0.92(2)}O_4$. The magnetic susceptibility shows a maximum at 16 K and Curie–Weiss behavior at higher temperatures, with $\mu_{eff}=5.11(4)$ $\mu_B$ per Mn atom. The susceptibility is consistent with spin-glass behavior: (i) the temperature at the susceptibility maximum is frequency-dependent and (ii) field cooled and zero-field cooled susceptibility curves differ below the maximum. Neutron powder diffraction data collected at 10 K does not show any sharp magnetic reflections, but a very broad reflection, with a full width at half maximum height of 7°, at a position corresponding to the 100 reflection is seen.

## Introduction

The preparation and characterisation of $MnTaO_4$ is part of a general investigation on phases formed in the Mn–Ta–O system[1] that have included studies of $Mn_4Ta_2O_9$ and $Mn_{11}Ta_4O_{21}$,[2] $Mn_3Ta_2O_8$,[3,4] $Mn_{0.6}Ta_{0.4}O_{1.65}$[5] and $Mn_{0.55}Ta_{0.45}O_{1.7}$.[6] A report of a $MnTaO_4$ phase exists in the literature,[7] but without any structure assignment or unit cell given, and no powder pattern for this phase exists in the JCPDS powder data bank, for example. There is also a report of a $MnNbO_4$ phase,[8] with a wolframite ($FeWO_4$) type structure, but a later investigation[9] shows that this claim is probably erroneous. Attempts by us to synthesize $MnTaO_4$ in an air or $O_2$ atmosphere at ambient pressure and temperatures below 1000 °C were not successful and yielded phases with Mn predominantly as $Mn^{2+}$. This article describes the synthesis of $MnTaO_4$ by a solid state reaction at high $O_2$ pressure and the characterization of its crystal structure and magnetic susceptibility.

## Experimental

$MnTaO_4$ was prepared by thoroughly grinding together manganese acetate tetrahydrate and fine-grained $Ta_2O_5$ and heating the mixture in air at 500 °C for 6 h. The pre-reacted powder was then reground, pelletised and heat-treated in a high-pressure chamber at 1050 °C under a total pressure of 10 kbar of a gas mixture of 20% $O_2$ in Ar for $2\times12$ h, with one intermediate regrinding.

A Guinier-Hägg camera with Cu-K$\alpha_1$ radiation was used for the collection of X-ray powder diffraction (XRPD) patterns for phase identification. The films were measured with a computer-controlled micro-densitometer. XRPD data for Rietveld refinements were collected with a STOE STADI/P diffractometer, using Cu-K$\alpha_1$ radiation and a linear position-sensitive detector covering 4.6° in 2$\theta$. Neutron powder diffraction (NPD) data were collected, both at room temperature and 10 K, at the Swedish research reactor R2 in Studsvik. The wavelength was 1.470 Å and the measured 2$\theta$ range 10–128°. The GSAS program package[10] was used for structure refinements.

Metal elemental analyses were carried out on a JEOL 820 SEM (scanning electron microscope) with the EDX (energy dispersive X-ray) analysis system LINK 10000.

The ac magnetic susceptibility was measured with a weak-field susceptometer (Lake Shore 7130) in the temperature range 10–300 K. Field cooled (FC) and zero-field cooled (ZFC) magnetization was measured with a vibrating sample magnetometer (VSM) equipped with a flowing gas cryostat. The VSM has a temperature resolution of 0.1 K and a field resolution of 0.1 mT.

## Results

### Compositional analysis

The crystallite size was estimated from SEM images to be 0.2–1.0 μm, see Fig. 1. EDX point analyses on individual grains

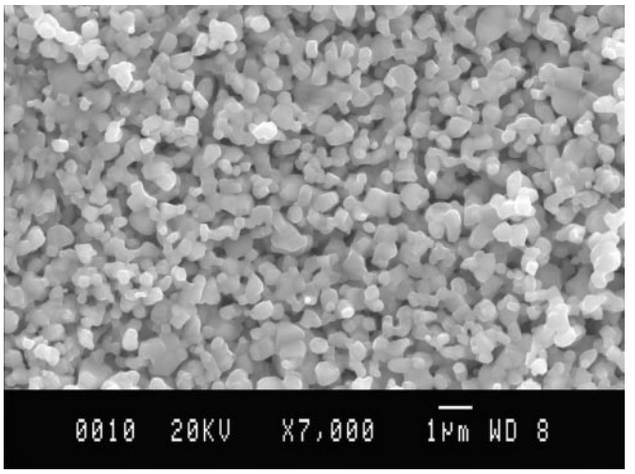


**Fig. 1** Secondary-electron SEM micrograph of $MnTaO_4$.

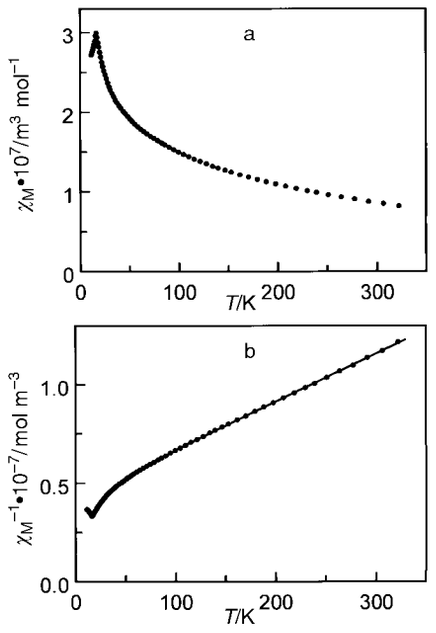


**Fig. 2** Molar magnetic susceptibility per Mn atom (a) and its inverse (b) *versus* temperature for $MnTaO_4$.

yielded a metal composition of 52(1)% Mn and 48(1)% Ta, indicating that the phase might contain a small amount of $Mn^{4+}$. The analysis results may, however, be subject to a systematic error due to the small crystallite size.

## Magnetic susceptibility

The magnetic susceptibility per Mn atom, $\chi_M$, of $MnTaO_4$ and its inverse, $\chi_M{}^{-1}$, are shown in Fig. 2 as functions of the temperature, $T$. The susceptibility shows a well-defined maximum at 16 K and Curie–Weiss law behaviour [$\chi_M = C/(T-\Theta)$] above *ca.* 100 K. The effective number of Bohr magnetons per Mn atom ($\mu_{eff}$) was determined from the Curie constant $C$ to be 5.11(4) $\mu_B$, which agrees with an expected value of 4.8–5.1 $\mu_B$ for $Mn^{3+}$ in a high-spin state, and $\Theta$ to be 175(1) K.

The maximum of the ac susceptibility was found to shift upwards in temperature with increasing measurement frequency (see Fig. 3), a behavior characteristic of a spin-glass,[11] with the shift proportional to the logarithm of the frequency by 0.223(1) K per decade. Measurements were also carried out using different frequencies between 8 and 4000 Hz, and different fields, at two temperatures, 15.5 and 17.2 K, on both sides of the maximum. Small, erratic, reproducible and, for both temperatures, coexisting signal variations with frequency were, however, present. The data were corrected for these, assuming them to be of instrumental origin, as has been done in Fig. 3, by scaling the data to the 500 Hz measurement at 17.2 K. The susceptibility at 17.2 K, *i.e.* above the maximum, is thereby tentatively also set to be frequency independent. The corrected 15 K data follow well a linear decrease of the susceptibility with the logarithm of the frequency by $2.54(7) \times 10^{-9}$ m$^3$ mol$^{-1}$ per decade. The linearity of the dependence partly justifies the applied correction, but does not rule out that a similar, but smaller, frequency dependence exists above the maximum.

Zero-field cooled (ZFC) and field cooled (FC) dc susceptibility curves measured in an applied magnetic field of 25 mT are shown in Fig. 4. The disparity of the two susceptibility curves below the transition temperature at 16 K is a further characteristic of a spin-glass.[11]

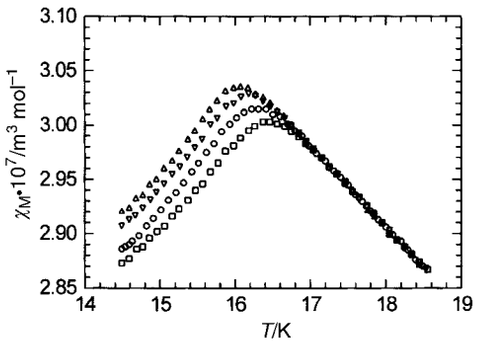


**Fig. 3** Molar magnetic ac susceptibility per Mn atom of $MnTaO_4$ at measuring frequencies 31.2 (□), 125 (○), 500 (▽) and 2000 Hz (△).

## X-Ray powder diffraction

The cell dimensions $a = 4.7189(3)$, $c = 2.9843(3)$ Å for rutile-type $MnTaO_4$ were obtained from Guinier-Hägg XRPD data, using Si as an internal standard and 14 reflections for $2\theta < 88°$. One very faint additional reflection showed that the sample contained a trace amount of $Mn_2O_3$.

## Structure refinements

XRPD data in the $2\theta$ range 25–127.5° was used in a Rietveld refinement which resulted in $\chi^2 = 0.95$, $R_{wp} = 2.9\%$, $R_p = 2.2\%$, $DwD = 0.77$ and $R_F = 3.8\%$. Three structural parameters were refined in space group $P4_2/mnm$: one positional parameter for the O atoms on the 4(*f*) sites ($x$,$x$,0) [$x$(O) = 0.3048(5)] and two isotropic displacement parameters, $U$(Mn/Ta) = 0.0044(2) and $U$(O) = 0.0013(1) Å$^2$. The powder pattern is shown in Fig. 5. The observed full width at half maximum height (FWHM) of the reflections was 0.23° at $2\theta = 62°$ and an estimation of the size of the scattering domains was calculated, using the Scherrer equation $t = 0.9\lambda/(B\cos\theta_B)$ and correcting for an instrumental width of 0.13°, to be *ca.* 500 Å.

A corresponding refinement from NPD data collected at room temperature and 51 reflections yielded $\chi^2 = 1.5$, $R_{wp} = 3.8\%$, $R_p = 3.0\%$, $DwD = 1.4$, $R_F = 2.6\%$, $x$(O) = 0.3077(1), $U$(Mn/Ta) = 0.006(2) Å$^2$ and $U$(O) = 0.0092(3) Å$^2$. A refinement of the metal composition significantly improved the fit between observed and calculated intensities and yielded a Mn content of 53.6(3)% Mn on the metal atom 2(a) sites (0,0,0), implying that the phase contains a small fraction of $Mn^{4+}$. Since metal losses during the synthesis are not likely to have occurred, this suggests an erroneous metal composition in the starting mixture used. The derived M–O distances (M = Mn/Ta) in the $MO_6$ octahedra are $2 \times 1.967(1)$ and $4 \times 2.052(1)$ Å.

NPD data were also collected at 10 K with the aim of determining a possible ordering of the magnetic moments. The data revealed, however, only a disordered magnetic structure (see below). A refinement of the nuclear structure at 10 K yielded the values $\chi^2 = 1.6$, $R_{wp} = 4.0\%$, $R_p = 3.1\%$, $DwD = 1.4$, $R_F = 1.8\%$, $x$(O) = 0.3078(1), $U$(Mn/Ta) = 0.002(2) Å$^2$, $U$(O) = 0.0064(3) Å$^2$ and 53.6(3)% Mn. The fit between observed and calculated patterns is shown in Fig. 6.

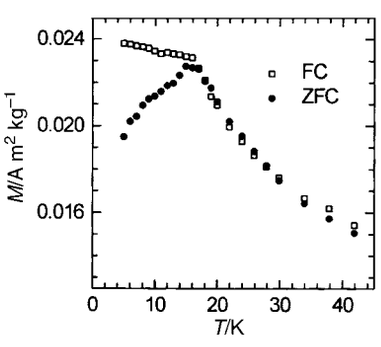


**Fig. 4** Field cooled (FC) and zero-field cooled (ZFC) dc susceptibility per Mn atom of $MnTaO_4$ at a field of 25 mT.

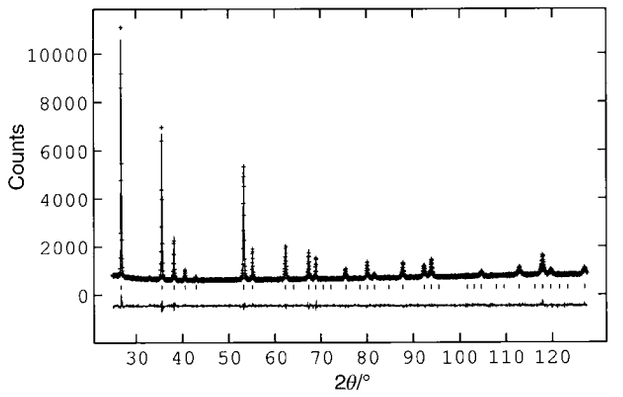


**Fig. 5** Observed, calculated and difference XRPD patterns of $MnTaO_4$.

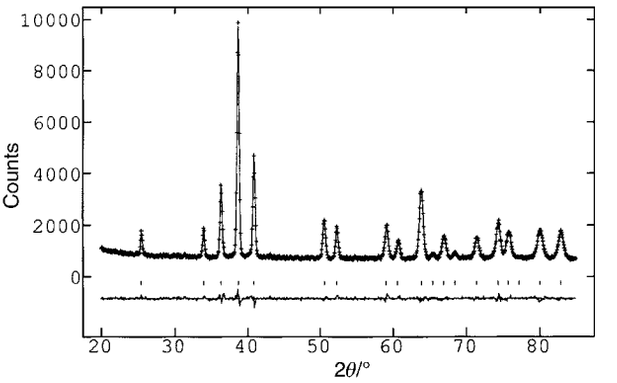


**Fig. 6** Observed, calculated and difference NPD patterns of $MnTaO_4$ at 10 K for $2\theta = 20$–$85°$.

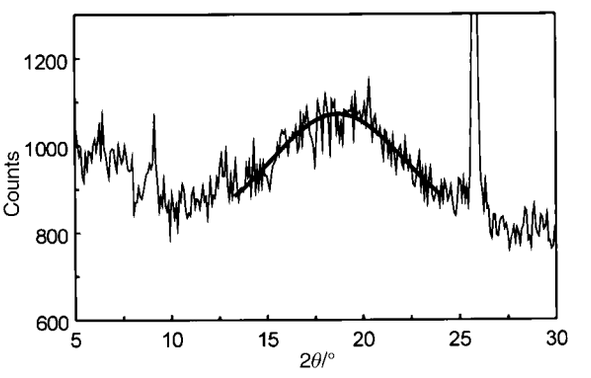


**Fig. 7** 10 K NPD data for $MnTaO_4$ showing the diffuse magnetic reflection at $2\theta \approx 18°$.

### Magnetic structure

The low-temperature 10 K NPD data show no Bragg peaks in addition to the nuclear ones. A very broad peak that indicates diffuse magnetic scattering is, however, evident at $2\theta \approx 18°$, as illustrated in Fig. 7. The peak is also present in the 295 K data but with a considerably weaker intensity. An approximate FWHM for this peak is 7°, corresponding to *ca.* 11 Å wide scattering domains.

The magnetic susceptibility data shows that $MnTaO_4$ behaves magnetically as a spin-glass. The magnetic properties can be compared with those of the compositionally similar and isostructural compound $FeTaO_4$.[12] The magnetic susceptibility of $FeTaO_4$ exhibits a broad maximum at *ca.* 25 K.[13,14] Below *ca.* 80 K, the susceptibility is found to be field-dependent and the transition has (based on this fact) been deduced to be that of a spin-glass.[14] NPD patterns collected at 2–140 K show only a diffuse magnetic scattering without any distinct transition.[12] At 4.2 K, a 1.2° broad peak is present that can be indexed as a 100 reflection[12] and this has been interpreted as indicating an anti-ferromagnetic ordering of the $MnF_2$ type, *i.e.* with spins aligned along the *c*-axis and those at the corner sites anti-parallel to the ones on the centre sites. The position of the diffuse magnetic peak observed at 10 K for $MnTaO_4$ is also close to that expected for a 100 reflection, 17.9°, which suggests a similarity in the magnetic structures of $MnTaO_4$ and $FeTaO_4$. The maximum for the magnetic susceptibility of $MnTaO_4$, at 16 K, is sharp however, contrary to that observed for $FeTaO_4$.

## Concluding remarks

The rutile structure is adopted by $M^{3+}Ta^{5+}O_4$ compounds with M = Ti, V, Cr, Fe, Al, Ga and Rh,[9,13–18] for which the ionic radii of $M^{3+}$ and $Ta^{5+}$ are (very) similar. Many of the compounds exhibit polymorphism. $GaTaO_4$[16] and $FeNbO_4$,[17,18] for example, also have modifications of the competing structure types of α-$PbO_2$ and wolframite ($FeWO_4$). The (disordered) rutile modification is usually the high-temperature/low-pressure form. It can be remarked that $FeTaO_4$, contrary to $FeNbO_4$, has so far only been reported with rutile,[12,18] tri-rutile[14] and, in small amounts, α-$PbO_2$-type[18] structures, implying different behavior for $FeNbO_4$ and $FeTaO_4$, despite the fact that Nb and Ta belong to the same group in the Mendeleev table. A comparison of *c*/*a* ratios and the *x*(O) parameter for $MnTaO_4$ and other rutile $MTaO_4$ phases shows that $MnTaO_4$ has a relatively lower *c*/*a* ratio, 0.632, and a larger *x*(O) parameter, 0.3075(2), compared with, respectively, 0.648–0.653 and 0.295–0.304 for the other phases. The $MO_6$ octahedra in $MnTaO_4$ are, thus, more regular.

$Mn^{3+}$ is a $d^4$ ion with the possibility of generating Jahn–Teller distortions. It is, therefore, somewhat surprising that $MnTaO_4$ does not adopt a rutile-related structure type[19] with $MO_6$ octahedra that have two longer and four shorter M–O bonds, though that would probably necessitate an ordering of the metal atoms.

The phases $MTaO_4$ with M = Ti, V, Cr show a paramagnetic temperature dependence of the magnetic susceptibility, while $FeTaO_4$ exhibits a broad maximum at *ca.* 25 K.[13,14] Similar diffuse NPD peaks are observed for $MnTaO_4$ and $FeTaO_4$,[12] which suggests similar local magnetic orderings.

It can finally be remarked that the ability to synthesize $MnTaO_4$ at a high oxygen pressure suggests the possibility of obtaining and investigating the magnetic properties of other isotypic phases, *e.g.* along the $MnO_2$–$MnTaO_4$–$MnTa_2O_6$ join or with two transition metals, such as $(Mn_{1-x}Fe_x)TaO_4$.

## Acknowledgements

This work has been financially supported by the Swedish Natural Science Foundation.

## References

1 S. Esmaeilzadeh, *Crystal Chemistry of Manganese Tantalum Oxides*, Doctoral dissertation, Department of Inorganic Chemistry, Stockholm University, 2000.
2 J. Grins and A. Tyutyunnik, *J. Solid State Chem.*, 1998, **137**, 276.
3 S. Esmaeilzadeh, J. Grins and A. Fitch, *J. Mater. Chem.*, 1998, **8**, 2493.
4 J. Grins, S. Esmaeilzadeh, P. Berastegui and S. Eriksson, *J. Mater. Chem.*, 1999, **9**, 1575.
5 S. Esmaeilzadeh, J. Grins and A.-K. Larsson, *J. Solid State Chem.*, 1999, **145**, 37.
6 S. Esmaeilzadeh, S. Lidin, M. Nygren and J. Grins, *Z. Anorg. Allg. Chem.*, 2000, **626**, 148.
7 A. C. Turnock, *J. Am. Ceram. Soc.*, 1966, **49**, 382.
8 H. Schröcke, *Beitr. Mineral. Petrogr.*, 1960, **7**, 166.
9 C. Keller, *Z. Anorg. Allg. Chem.*, 1962, **318**, 89.

10 A. C. Larson and R. B. Von Dreele, Los Alamos National Laboratory Report No. LA-UR-86-748, 1987.
11 J. A. Mydosh, *J. Magn. Magn. Mater.*, 1996, **157/158**, 606.
12 H. Langhof, H. Weitzel, E. Wölfel and W. Scharf, *Acta. Crystallogr., Sect. A*, 1980, **36**, 741.
13 D. N. Ostrov, N. A. Kryukova, R. B. Zorin, V. A. Makarov, R. P. Ozerov, F. A. Rozhdestvenskii, V. P. Smirnov, A. M. Turchaninov and N. V. Fadeeva, *Sov. Phys. Crystallogr. (Engl. Transl.)*, 1973, **17**, 1017.
14 A. Nørlund Christensen, T. Johamsson and B. Lebech, *J. Phys. C: Solid State Phys.*, 1976, **9**, 2601.
15 K. Brandt, *Ark. Kemi, Mineral. Geol.*, 1943, **17A**, 15.
16 G. Bayer, *Ber. Dtsch. Keram. Ges.*, 1962, **39**, 535.
17 R. S. Roth and J. L. Waring, *Am. Mineral.*, 1964, **49**, 241.
18 G. Pourroy, A. Malats, I. Riera, P. Poix and R. Poinsot, *J. Solid State Chem.*, 1990, **88**, 476.
19 W. H. Bauer, *Z. Kristallogr.*, 1994, **209**, 143.